Journal of Scientific Research & Reports
6(2): 84-98, 2015; Article no.JSRR.2015.134
ISSN: 2320-0227

SCIENCEDOMAIN
SCIENCEDOMAIN *international*
www.sciencedomain.org

Numerical Analysis of Semiconductor PN Junctions Using MATLAB^{TM}

Hamid Fardi[1*]

[1] *Department of Electrical Engineering, University of Colorado Denver, United States of America.*

Author's contribution

The sole author designed, analyzed and interpreted and prepared the manuscript.

Article Information

DOI: 10.9734/JSRR/2015/14434
Editor(s):
(1) José Alberto Duarte Moller, Center for Advanced Materials Research, Complejo Industrial Chihuahua, Mexico.
Reviewers:
(1) Yoshiki Yonamoto, Hitachi, Ltd., Yokohama Laboratory, Japan.
(2) Jyh Jian Chen, Department of Biomechatronics Engineering, National Pingtung University of Science and Technology, Taiwan.
(3) Abel Garcia-Barrientos, Electronics and Computer Science Dept., Autonomous University of Hidalgo State (UAEH), México.
Complete Peer review History: http://www.sciencedomain.org/review-history.php?iid=963&id=22&aid=8080

Original Research Article

Received 30th September 2014
Accepted 13th January 2015
Published 7th February 2015

ABSTRACT

The purpose of this project is to develop a functional PN semiconductor device simulator that is modular in nature in order to allow for flexibility during programming and to allow for future development with relative ease. In addition, the program's main goal is to provide a tool that can supplement device modeling and the standard course material covered in a basic college level introduction, semiconductor device physics, course or and numerical analysis course and to construct basic PN semiconductor devices which can be studied using standard numerical analysis techniques. A device modeling program is developed using the basic MATLAB tools necessary to understand the operation of the program and allow future developments as necessary. MATLAB's capability and inherent nature of handling matrices and matrix operations makes this approach an excellent technique to develop numerical analysis algorithms.

The program solution will be used to examine device parameters such as carrier statistics, device potential, and internal electric fields. The device solution is compared to analytical approximations in order to further strengthen the understanding between theory and exact numerical solutions and how those solutions are obtained.

Keywords: Device simulation; MATLAB; semiconductors; numerical analysis.

**Corresponding author: Email: Hamid.Fardi@ucdenver.edu;*

1. INTRODUCTION

The purpose of this project is to develop a general purpose semiconductor device simulator (SDS) that is functional and modular in nature in order to allow flexibility and future development without any major reprogramming effort to the base code. In addition, the program's main goal is to develop a tool that can supplement the standard course material covered in a basic college level Introduction to Semiconductor Physics course, or Numerical Analysis course to build basic semiconductor devices and study the various parameters such as carrier statistics, device potential, and internal electric fields [1,2].

Although there are several industry and student level device physics simulators already available [3], the hope is that with this new tool and report, the theory of numerical analysis applied to device physics can be studied in a more thorough manner. The addition of the report that supplements the program will develop the basic tools necessary to understand the operation of the program and allow future developments as necessary.

This project was developed in the programming environment provided by MATLAB™ which is developed and supported by Mathworks [4]. Almost all academic institutions use MATLAB heavily in the learning process and is readily available to most students, hence the choice of this programming environment. Additionally, MATLAB is an extremely powerful numerical analysis tool that makes the solution of a program like this one rather straightforward. MATLAB's capability and inherent nature of handling matrices and matrix operations makes this an excellent tool to develop numerical analysis algorithms [5].

The current semiconductor simulation tools available do not lend to updates or modification simple or straightforward. In fact most tools are not open to be changed in any manner unless the source code is available [6]. With the open nature of MATLAB the solution process can be studied throughout and all variables and parameters are available to study. The program does have the capability to be standalone which allows for the use of the tool without the requirement of the MATLAB environment [7-15].

The remaining discussion in this section gives a brief overview of the contents included in this report.

Section 2 gives a brief introduction to the devices physics required to build a numerical analysis program to simulate semiconductor devices in general. Device physics equations (continuity, poisson's, current, etc.) are discussed as are the models, such as mobility, SRH (Shockley-Read Hall) Recombination, and generation. Boundary conditions are also discussed. Lastly, silicon material parameters are given and briefly discussed. Currently no other semiconductor material is used in this program, but the addition of other materials is rather straightforward.

Section 3 will give a brief introduction to numerical analysis techniques followed by simulation results in section 4 and compare them to basic theory (depletion width, built in potential, etc.) as well as with other simulation tools, such as Sim Windows.

APPENDIX – This section will discuss the program as written and the various functions built to support it. Each function will be discussed and explained. It should be noted however, that the MATLAB code itself is heavily commented as a supplement to this section.

2. SEMICONDUCTOR DEVICE PHYSICS

Semiconductor device phenomenon is described and governed by Poisson's equation (1)

$$\begin{aligned}&\frac{\partial^2\psi}{\partial\, x^2} = -\frac{q}{\varepsilon_s}(\Gamma + p - n)\\&where, \Gamma = N(x) = N_d - N_a\end{aligned} \qquad (1)$$

Is the effective doping concentration defined for the semiconductor, *N(x)* is the position dependent net doping density, *Nd* is the donor density, and *Na* is the acceptor density. Equation (1) is the differential equation for the potential distribution in an arbitrarily doped semiconductor [16-18]. This equation, depending upon the particulars, is difficult to solve analytically and in some cases can be impossible. Approximations must be made in most analytical solutions, alternatively numerical methods can be used which is the focus of this report. The time (*t*) dependent equations for electrons and holes (2a,b) are defined by electron (n) and hole (p) densities, electron current density (J_n) and hole current density (J_p).

$$\frac{\partial n}{\partial t} - \frac{1}{q} div J_n = G - (U_{b-b} + U_{SRH}) \quad (2a)$$

$$\frac{\partial p}{\partial t} + \frac{1}{q} div J_p = G - (U_{b-b} + U_{SRH}) \quad (2b)$$

Equations (2a) and (2b) are known as the continuity equations for electrons and holes respectively. In equation (2), *q* is the electronic charge, G is the total generation rate per unit volume, U_{b-b} is the band-to-band radiative recombination rate per unit volume, and U_{SRH} is the Shockley-Read-Hall recombination rate per unit volume [19,20]. It is assumed that the recombination centre is at the middle of the bandgap energy level. This assumption simplifies the Shockly-Read-Hall recombination model to be dependent on only the carriers lifetime.

These equations are used to describe the free carrier densities and their properties within the device by examining their interactions within a small infinitesimal volume that we can extend across the device as a whole. The current transport equations or current densities are defined by a combination of the drift and diffusion affects on the free carriers within the device. The drift portion of the current expression is simply due to the presence of an electric field (*E*), if there is one. This electric field creates an overall drift velocity v_d, and is proportional to the electric field and the mobility of the carrier [21-23].

$$v_d = -\mu_n E \quad (3)$$

The mobility (μ_n) of the electron carrier is a parameter that describes the ease of motion of an electron in response to an electric field.

The same procedure can be extended to the hole free carriers and then combined to give the total current density due to the applied electric field in equation (4).

$$J_{drift} = J_{n,drift} + J_{p,drift} = (q\mu_n n + q\mu_p p)E \quad (4)$$

In Eq. (4) J_{drift} is the total drift current density, $J_{n,drift}$, and $J_{p,\ drift}$ are the drift current densities of the free carriers, and the hole carrier mobility is defined by μ_p. The other affect on the current density through a device is due to the diffusion of free carriers in the device if a special variation of carrier energies or densities exist.

$$J_{n,diff} = qD_n \frac{dn}{dx} \quad \text{where,} \quad D_n = \frac{kT}{q}\mu_n \quad (5)$$

The quantity D_n, is known as the diffusion constant or Einstein relationship. In Eq. (5) *k* is the Boltzmann constant and the ambient temperature is defined by *T* in unit of Kelvin.

2.1 Carrier Densities

The carrier models used in this program follow the Boltzmann statistics approximation.

This project neglects band gap narrowing due to heavy doping levels. The intrinsic carrier concentration (n_{ie}) then is only modeled as a function of temperature as shown below.

$$n_{ie}(T) = \sqrt{N_C(T) N_V(T)} \exp\left(-\frac{E_g(T)}{2kT}\right) \quad (6)$$

N_C *(T)* and N_V *(T)* are known as the density of states for conduction and valence bands and along with the band-gap energy, E_g also have dependencies on temperature (*T*) [24-27].

$$E_g(T) = E_g(300) + \alpha\left[\frac{300^2}{300+\beta} - \frac{T^2}{T+\beta}\right] \quad (7)$$

$$N_C(T) = \left(\frac{T}{300}\right)^{3/2} \cdot N_C(300) \quad (8)$$

and

$$N_V(T) = \left(\frac{T}{300}\right)^{3/2} \cdot N_V(300) \quad (9)$$

$N_C(300)$ and $N_V(300)$ along with α and β, are predefined constant quantities given in Table 1.

Currently only parameters for Silicon material are used. The corresponding program variable is also shown in Table 1.

2.2 Mobility Models

The mobility (μ) of an electron or hole to move throughout the silicon crystal lattice is representation of the responsiveness of a free carrier to move through the conduction and valence bands in the presence of an electric field. This phenomenon is governed by several complex interactions at the quantum mechanical level [28,29].

Temperature plays a major role because at higher temperatures the lattice will vibrate more causing the overall free carrier mobility to lower. Dopant levels also have a significant role since the dopant sites create local distortions in the lattice allowing the free carriers to scatter more [30].

The models built into SDS allow for effective doping dependency and electric field dependency. There is also a factor included to take into account for high-injection levels in high power devices. These models can be turned on or off to account for any dependency that is desired.

$$\mu = \left[\frac{\mu_{\max} - \mu_{\min}}{1 + \left(\frac{|N(x)|}{N_{ref}} \right)^{\alpha} + f} + \mu_{\min} \right] \cdot \frac{1}{\left[1 + \left(\frac{E}{E_c} \right)^{\beta} \right]^{1/\beta}} \qquad (10)$$

where,

$$f = \left(\frac{np^{1/2}}{2.04 N_{ref}} \right)^{\alpha} \qquad (11)$$

The $\mu_{\max}$, $\mu_{\min}$, N_{ref}, α, β, and E_c are constants and fitting parameters tabulated in Table 2.

The SDS program models both generation and recombination for use in determining current flow in the specified device when solving both the continuity equations and Poisson's equation. The most fundamental type of recombination defined as Shockley-Read Hall recombination (U_{SRH}). The recombination rates are defined as:

$$U_{SRH} = \frac{np - n_{ie}^2}{(p + n_{ie})\tau_n + (n + n_{ie})\tau_p}, \qquad (12)$$

Table 1. Material parameters for silicon

Nomenclature	Physical parameter	MATLAB program variable	Default value	Units
Relative permittivity	ε_r	er	11.7	-
Silicon permittivity	ε_s	es	1.036×10^{-12}	F/cm
Energy gap (300K)	E_g (300)	EG300	1.08	eV
Alpha	α	EG_alpha	4.73×10^{-4}	-
Beta	β	EG_beta	636	-
Conduction band density of states (300K)	N_C	NC300	2.8×10^{19}	cm^{-3}
Valence band Density of states (300K)	N_V	NV300	1.04×10^{19}	cm^{-3}
Electron mobility	μ_n	Function	1350	cm^2/V-sec
Hole mobility	μ_p	Function	495	cm^2/V-sec
Intrinsic carrier concentration	n_{ie}	nie	1.45×10^{10}	cm^{-3}
SRH electron lifetime	τ_n	tau_n0	0.2×10^{-7}	sec
SRH hole lifetime	τ_p	tau_p0	0.2×10^{-7}	sec
Donor energy level		-	0.044	eV
Acceptor energy level		-	0.045	eV
Saturation velocity		Function	-	cm/sec
Band-to-Band constant, *B*		-	2.8×10^{-31}	cm^6/sec

where, n_{ie} is the intrinsic carrier density at thermal equilibrium.

The electron and hole lifetime are defined by τ_n and τ_p, respectively and are defined below where σ, is the capture cross-section for electrons (σ_n) and holes (σ_p), N_t is the density of trapping centers, and V_{th} is the thermal velocity.

$$\tau_n = \frac{1}{\sigma_n v_{th} N_t} \quad and \quad \tau_p = \frac{1}{\sigma_p v_{th} N_t} \tag{13}$$

It is assumed that the recombination center is located at the middle of the band gap energy level. This assumption simplifies the Shockley-Read-Hall recombination model to be dependent on only the carriers lifetime.

The band-to-band recombination ($U_{b\text{-}b}$) is characterized by electron-hole pairs disappearing without the aid of trapping centers modeled in equation (2) by $U_{b-b} = B(np - n_{ie}^2)$.

The generation term *(G)* used in this program models the basic generation affect due to impact ionization rate for electrons (α_n) and holes (α_p). It is useful in characterizing reverse applied bias breakdown. In low electric field applied bias cases the generation rates are typically negligible.

$$G = G_n = G_p = \frac{1}{q}\left(\alpha_n \left|J_n\right| + \alpha_p \left|J_p\right|\right) \tag{14}$$

Where,

$$\alpha_n = \alpha_{n0} \exp\left(-\left(\frac{E_{n0}}{|E|}\right)^m\right) \quad and \quad \alpha_p = \alpha_{p0} \exp\left(-\left(\frac{E_{p0}}{|E|}\right)^m\right) \tag{15}$$

The constants α_{n0}, α_{p0}, E_{n0}, E_{p0}, and *m* are tabulated in Table 3.

Table 2. Mobility parameters

Nomenclature	Physical parameters	MATLAB program variable	Default value	Units
Electron mobility concentration reference	$N_{ref,n}$ in Eq. (10)	Nrefn	8.5 x 10^{16}	cm^{-3}
Electron mobility alpha	*α* in Eq. (11)	alphan	0.72	-
Electron mobility beta	*β* in Eq. (10)	betan	2	-
Electron critical electric field	*Ec*	Ecn	8.0 x 10^3	V/cm
Electron maximum mobility	μ_{max}	mu_maxn	1330	cm^2/V-sec
Electron minimum mobility	μ_{min}	mu_minn	65	cm^2/V-sec
Hole mobility concentration reference	$N_{ref,p}$ in Eq. (10)	Nrefp	6.3 x 10^{16}	cm^{-3}
Hole mobility alpha	*α* in Eq. (11) for hole	alphap	0.72	-
Hole mobility beta	*β* in Eq. (10) for hole	betap	1	-
Hole critical electric field	*Ec* for hole	Ecp	1.95 x 10^4	V/cm
Hole maximum mobility	μ_{max} for hole	mu_maxp	495	$cm^{2/}$V-sec
Hole minimum mobility	μ_{min} for hole	mu_minp	47.7	cm^2/V-sec

Table 3. Generation parameters

Nomenclature	Physical parameter	MATLAB program variable	Default value	Units
Electron Alpha	α_n in Eq. (14)	alpha_n0	2.25 x 10^7	
Hole Alpha	α_p in Eq. (14)	alpha_p0	3.08 x 10^6	
Electron Energy	E_{n0} in Eq. (15)	E_n0	3.26 x 10^6	V/cm
Hole Energy	E_{p0} in Eq. (15)	E_p0	1.75 x 10^6	V/cm
Fitting Parameter	*m* in Eq. (15)	m	1	-

3. NUMERICAL ANALYSIS

The electrical device equations are solved by direct Newton-Raphson's method and the energy balance equations are solved by Gummel's decoupled method [31]. This approach is implemented due to its simplicity in modifying an existing simulation program [32]. The isothermal electrical equations are solved for fundamental variables of quasi-Fermi levels for electrons and holes and electrostatic potential at a preconditioned electron temperature (the lattice temperature is kept at an ambient room temperature). For non-isothermal conditions, Gummel's method is used to compute electron temperature. Two types of boundary conditions: Ohmic contacts and finite surface recombination velocity are supported. Standard box discretization method of both the carrier continuity equations and the energy balance equations are applied by extending Scharfetter-Gummel algorithm, similar to those used in the literature [18,19].

3.1 P-N Junction Diode Example

In this section, a procedure for performing DC analysis of a 1-D, P-N junction device will be developed. The basic P-N junction diode is examined as further development techniques for other devices follow the same basic procedures and solutions used in this section. For a 1-D Bipolar Junction Transistor, for example, only slight modification of this procedure is required and the resulting simulator program can be modified to use either solution depending upon the device specified. Another example of modification is time domain analysis, which requires extra division spacing but ultimately requires little modification to the base program with the conceptual idea that these further implementations can be readily incorporated.

Before we can proceed with numerical analysis of the device shown in Fig. 1, a few points of interest should be noted. Many of the models used in the solution procedure can be expanded easily to incorporate more advanced models. For example, the intrinsic carrier concentration model is currently only temperature dependent and the mobility model is fixed across the device. Both could be modified to incorporate band gap narrowing for heavily doped devices or electric field dependency respectively. More discussion on each model used in this section along with its capabilities is further discussed in Section 4.

The boundary conditions need to satisfy a zero space charge region at each contact *x=0* and *x=w* as shown in Fig. 2. Usually the semiconductor forming an ohmic contact with the metal has sufficiently high doping concentration. If there were a nonzero space charge region in such a highly doped semiconductor, then there would be a correspondingly high electric field which would lead to breakdown conditions at the metal-semiconductor contact, so therefore the zero space charge condition must be satisfied.

$$\Gamma(0) + p(0) - n(0) = 0, \quad \Gamma(w) + p(w) - n(w) = 0, \tag{16a}$$

$$p(0)n(0) = n_i^2, \quad p(w)n(w) = n_i^2, \tag{16b}$$

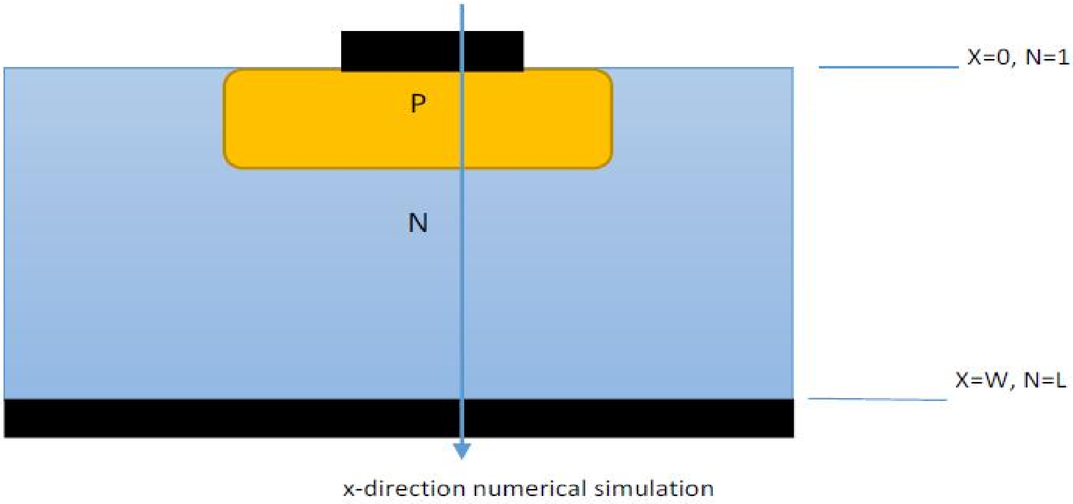

Fig. 1. Schematic of a P-N junction diode at x-direction

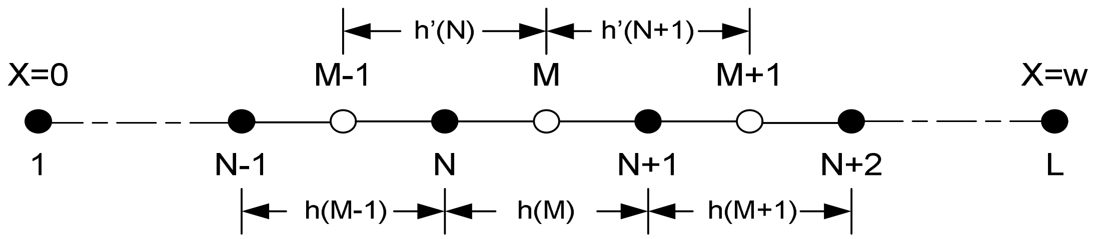

Fig. 2. Division points for dc analysis

$$\psi(0) = V - \frac{1}{\theta}\ln\left[\frac{p(0)}{n_i}\right], \quad \psi(w) = V - \frac{1}{\theta}\ln\left[\frac{n(w)}{n_i}\right], \quad where, \quad \theta = \frac{q}{kT} \tag{16c}$$

Equation (16a) satisfies the zero space charge condition specified above, while equation (16b) satisfies the thermal equilibrium condition necessary at each contact. Equations (16a and b) are used to establish the two-point boundary conditions that are self-consistent among the two equations and the result is shown in equation (17).

$$\begin{aligned} p(0) &= -\frac{\Gamma(0)}{2}\left\{1+\left[1+\left(\frac{2n_i}{\Gamma(0)}\right)^2\right]^{1/2}\right\}, \quad n(0) = \frac{n_i^2}{p(0)} \\ n(w) &= -\frac{\Gamma(w)}{2}\left\{1+\left[1+\left(\frac{2n_i}{\Gamma(w)}\right)^2\right]^{1/2}\right\}, \quad p(w) = \frac{n_i^2}{n(w)} \end{aligned} \tag{17}$$

Conditions for the potential boundary conditions given in equation (16c) are deduced by the use of the quasi-Fermi potentials briefly discussed in Section 2. These are re-written here in equation (18) for reference.

$$\psi = \phi_p - \frac{1}{\theta}\ln\left[\frac{p}{n_i}\right], \quad \psi = \phi_n - \frac{1}{\theta}\ln\left[\frac{n}{n_i}\right], \quad where, \quad \theta = \frac{q}{kT} \tag{18}$$

If the definition of the zero potential point on the n-region and applied bias (*V*) on the p-region is extended to equation (18) it follows that

$$\phi_p(w) = \phi_n(w) = 0 \quad and \quad \phi_p(0) = \phi_n(0) = V$$

. With equation (17c) and equation (18) we now have a two-point boundary condition with respect to the three unknown variable, n, p, and ψ for use in the solution of the device.

This solution uses uniform mesh spacing and is sufficient for most classes of devices, however when the extent of the depletion region becomes much smaller than the neutral bulk regions it is sometimes more beneficial to have course mesh spacing in the neutral regions and finer mesh spacing in the depletion region.

3.2 Numerical Solution

This section will discuss the numerical solution process used to solve the matrix-vector equation (33), including development of the trial values, or initial guess, and finally Newton's iteration principle to update the trial values and check for convergence of the solution.

A solution procedure is conceptualized below:

(1) Define physical and numerical parameters
(2) Define iteration limit and set current iteration number to zero.
(3) Use the matrix-vector coefficients to calculate the error for each iteration using the recursive algorithm discussed in Appendix.
(4) Improve the initial guess or trial potentials by adding the calculated error.
(5) Check for convergence against defined convergence tolerance.
(6) End program if solution has converged otherwise update current iteration limit by 1 and return to step (3) repeating the process until solution has converged or iteration limit is reached.

Assuming that a converged solution for the equilibrium condition has been reached, extending the solution to an external biased condition only requires updating the equilibrium condition potential with a simple proportional relationship and then repeating the process defined above. The numerical constants and the physical constants are given in Table 4 and Table 5 respectively.

4. SDS RESULTS INVESTIGATED

In this section, we will review the output of the SDS program and compare it to other simulators, notable SimWindows [6]. SimWindows is also a 1-D semiconductor device simulator capable of simulating the same devices as the SDS program.

Fig. 3. shows the output for the potential of the SDS program when run with an abrupt step junction of equal doping in both regions. The cursor in the graph is displaying the pertinent information.

We can also observe in Fig. 3 that the potential is zero at the junction transition as we expect since the doping densities are equal in the bulk n and p-regions. Fig. 4 shows the equilibrium electric field throughout the device. It is also symmetrical about the junction as we expect.

Figs. 5 and 6 show the potential for a PN junction where the acceptor dopant density is greater than the donor density. This shows the depletion region extending further into the n-region as it should, as well as a nonzero value at the transition region. Fig. 6 is taken from SimWindows as verification the correct solution was obtained. The only difference in SimWindows is that all plots are scaled to zero, meaning there are no negative potential values. SDS has an option to do this as well and the result is shown in Fig. 7.

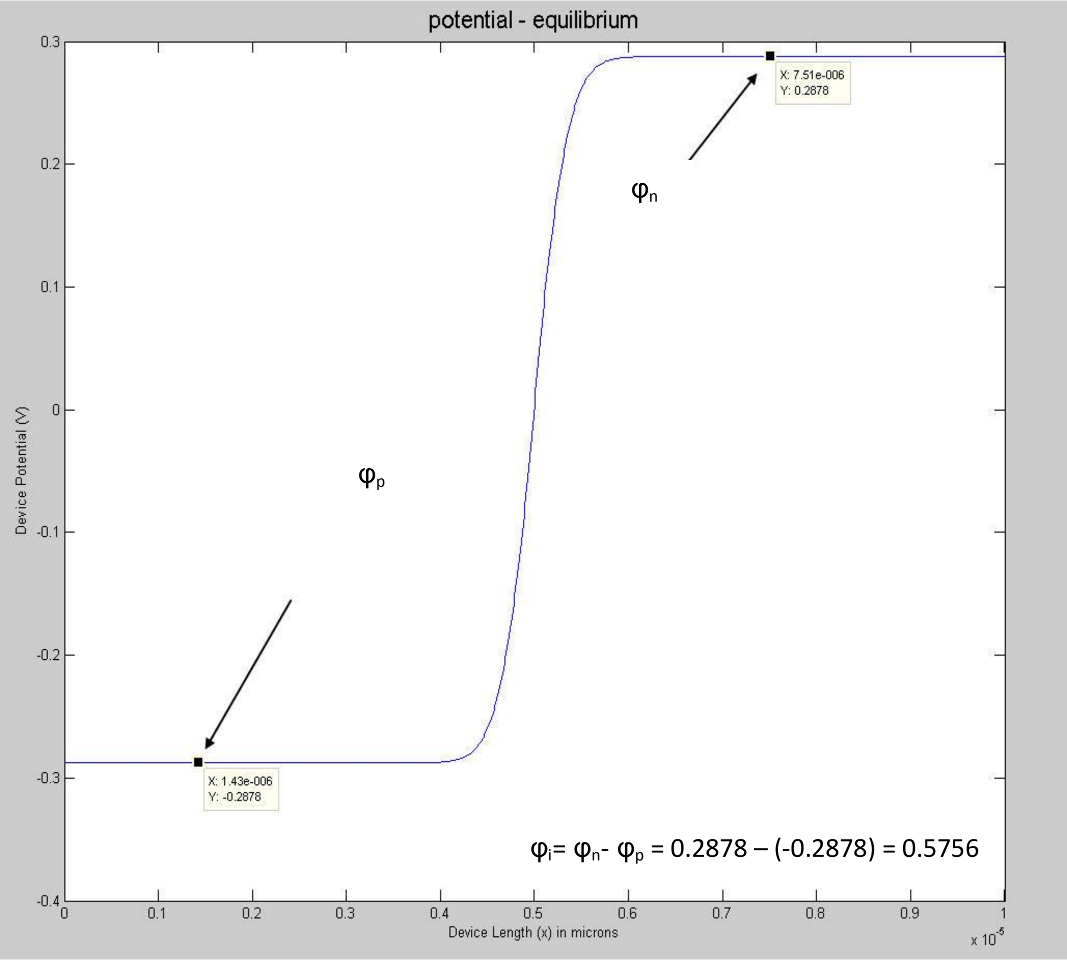

$\varphi_i = \varphi_n - \varphi_p = 0.2878 - (-0.2878) = 0.5756$

Fig. 3. Equilibrium device output potential

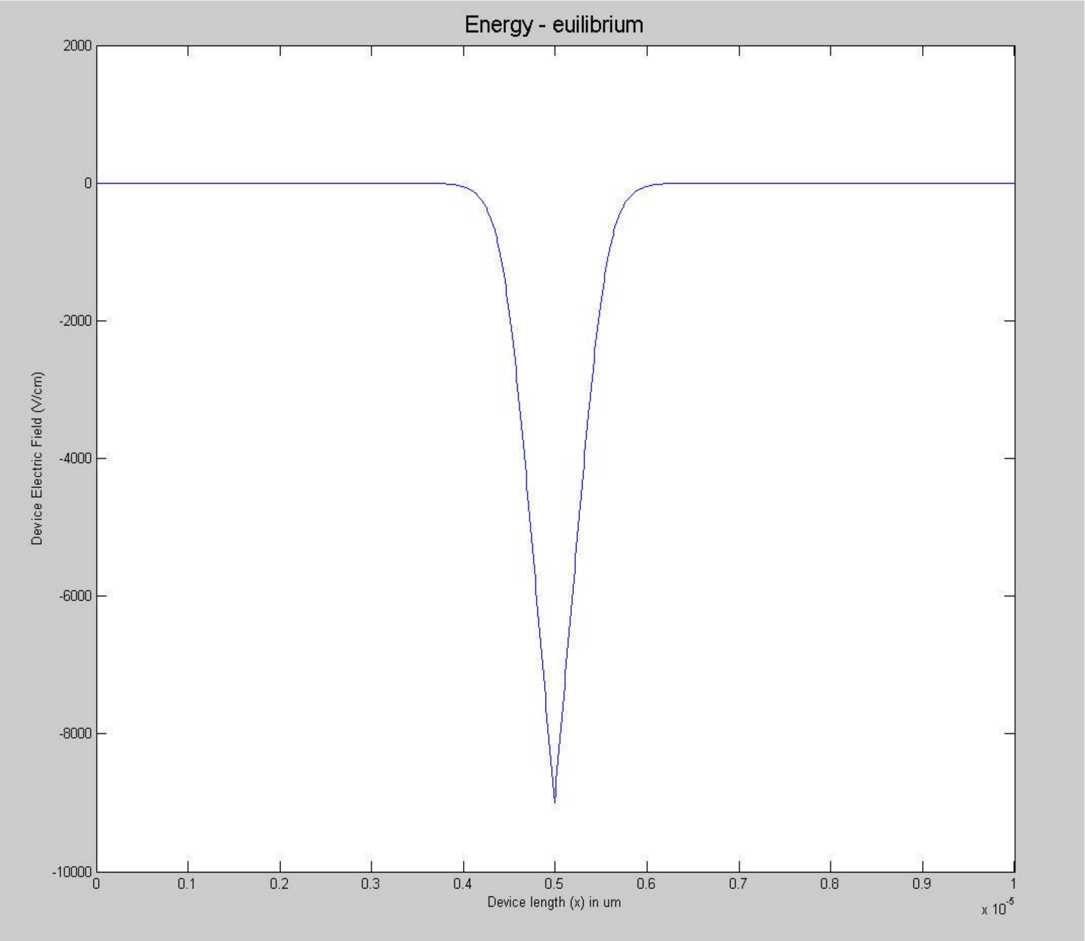

Fig. 4. Equilibrium electric field. Emax is at the transition region.

Table 4. Numerical constants

Nomenclature	MATLAB program variable	Default value	Units
Device length	length	10	um
Convergence tolerance	etol	1 x 10-6	-
# Grid points	L	1001	-
Iteration number	it	0	-
Iteration limit	itl	15	-

Table 5. Physical constants

Nomenclature	Program variable	Default value	Units
Dielectric permittivity constant	*eo*	8.854 x 10^{-14}	F/cm
Electronic charge	*q*	1.602 x 10^{-19}	C (A-sec)
Boltzmann's constant	*k*	8.62 x 10^{-5}	eV/K
Thermal voltage	*Vt*	0.02586	V
Boltzmann factor (thermal voltage)	*1/Vt*	38.6	1/V
Temperature	*T*	300	K
Donor concentration	*Nd*	1 x 10^{15}	cm^{-3}
Acceptor concentration	*Na*	1 x 10^{15}	cm^{-3}
Left contact	*Vl*	0	V
Right contact	*Vr*	0	V

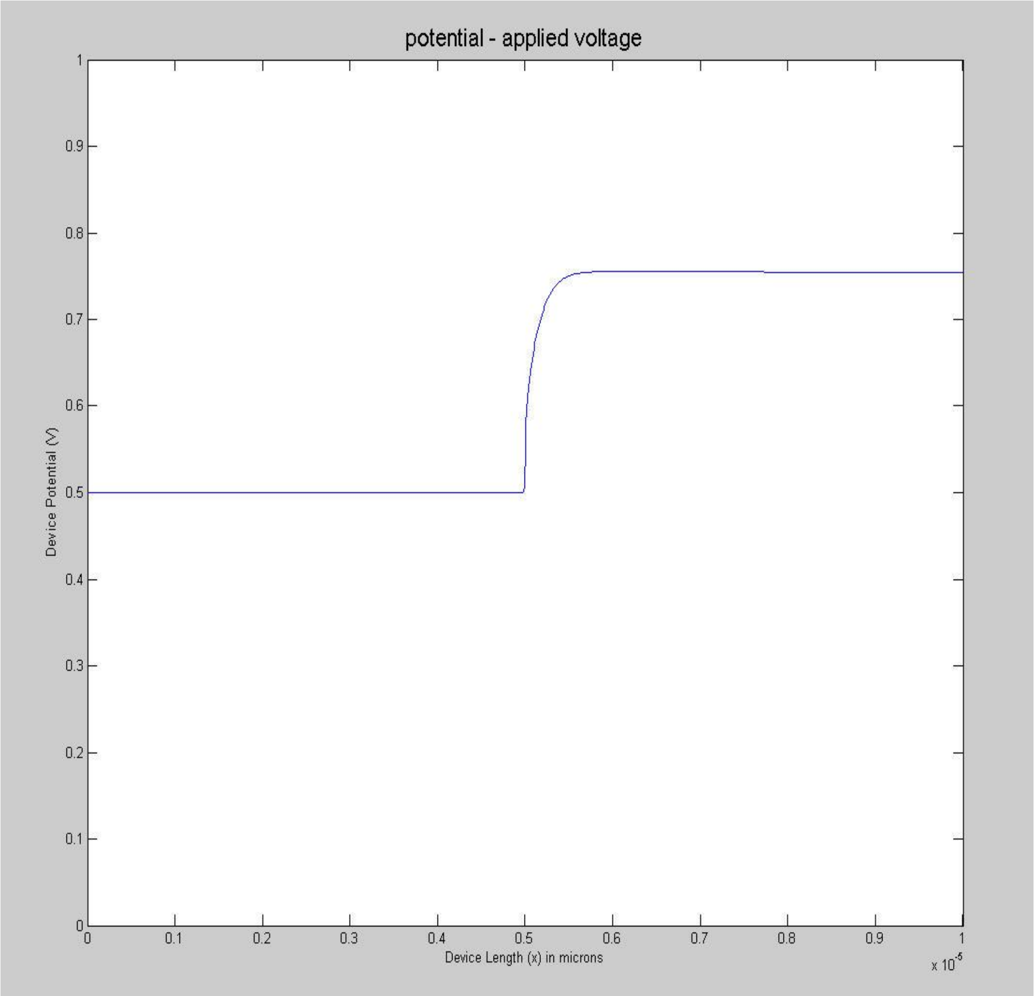

Fig. 5. Equilibrium device potential with external applied bias

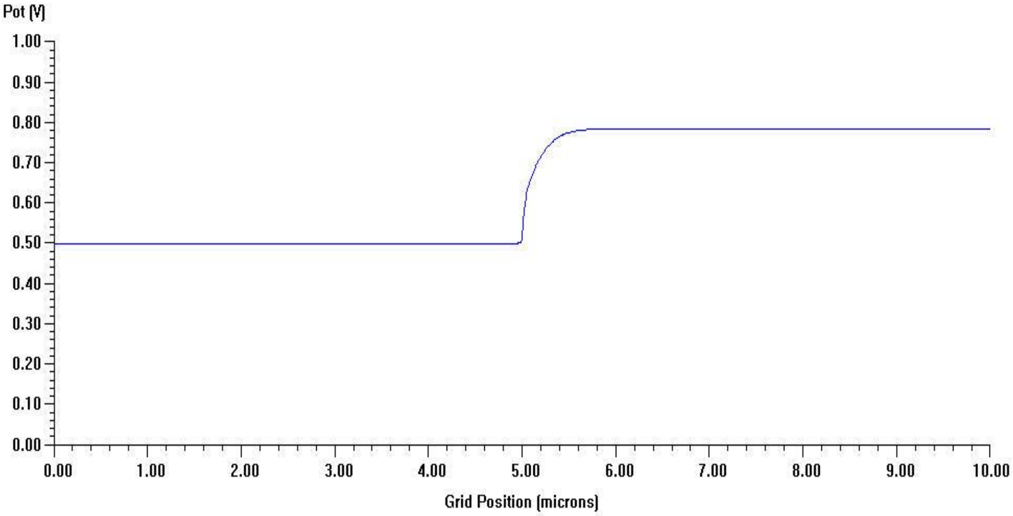

Fig. 6. SimWindows comparison to Fig. 5 with external applied bias

Fig. 8 shows the electric filed simulation using SimWindows. The electric field comparison with SimWindows using SDS program is shown in Fig. 9. The electric field is always max at the junction transition; however when the dopant densities are unequal across the junction, the field will be push further into the region with less doping atoms just as the depletion region does.

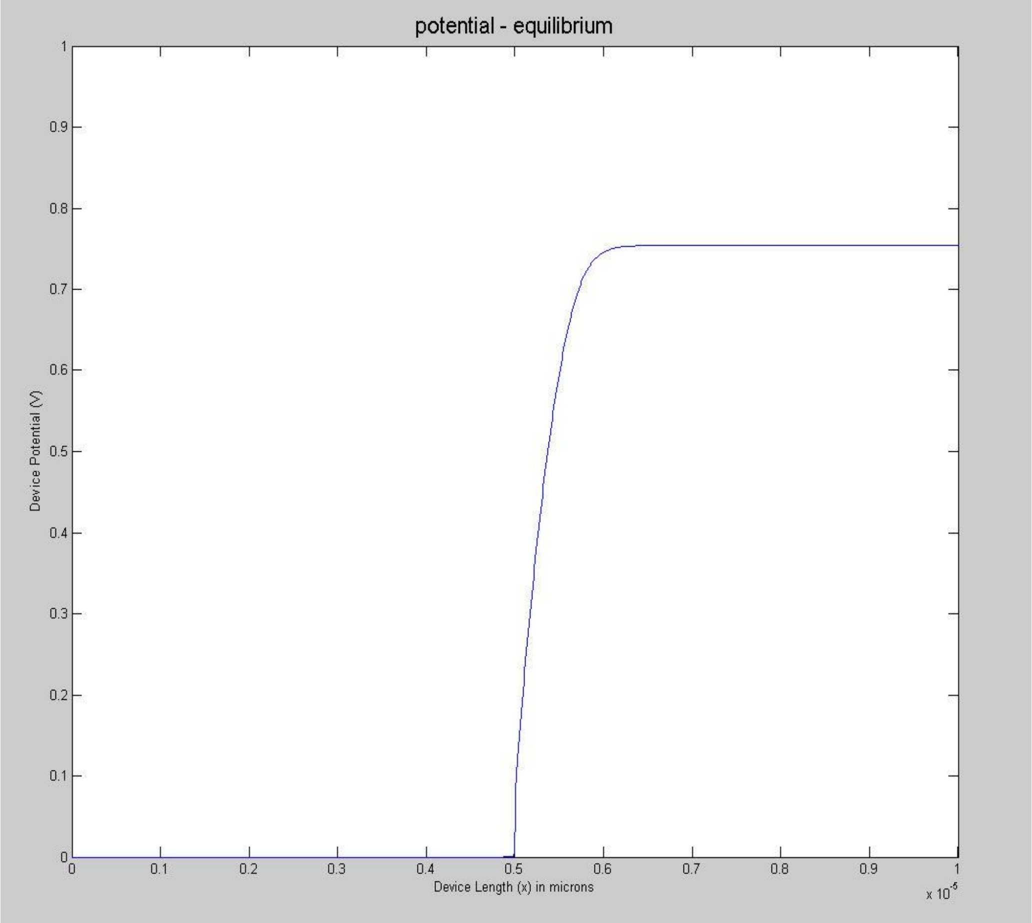

Fig. 7. SDS output shifted to zero as compared to Fig. 6

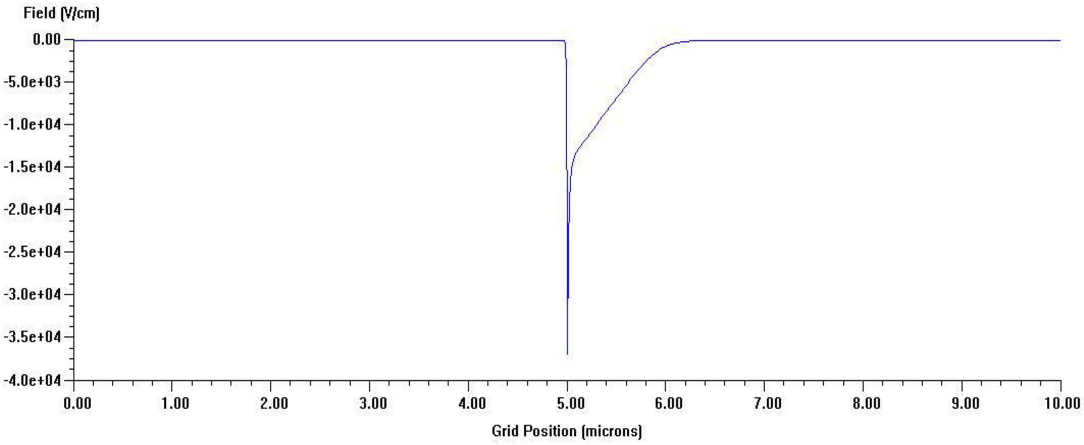

Fig. 8. Electric field simulation obtained using SimWindows

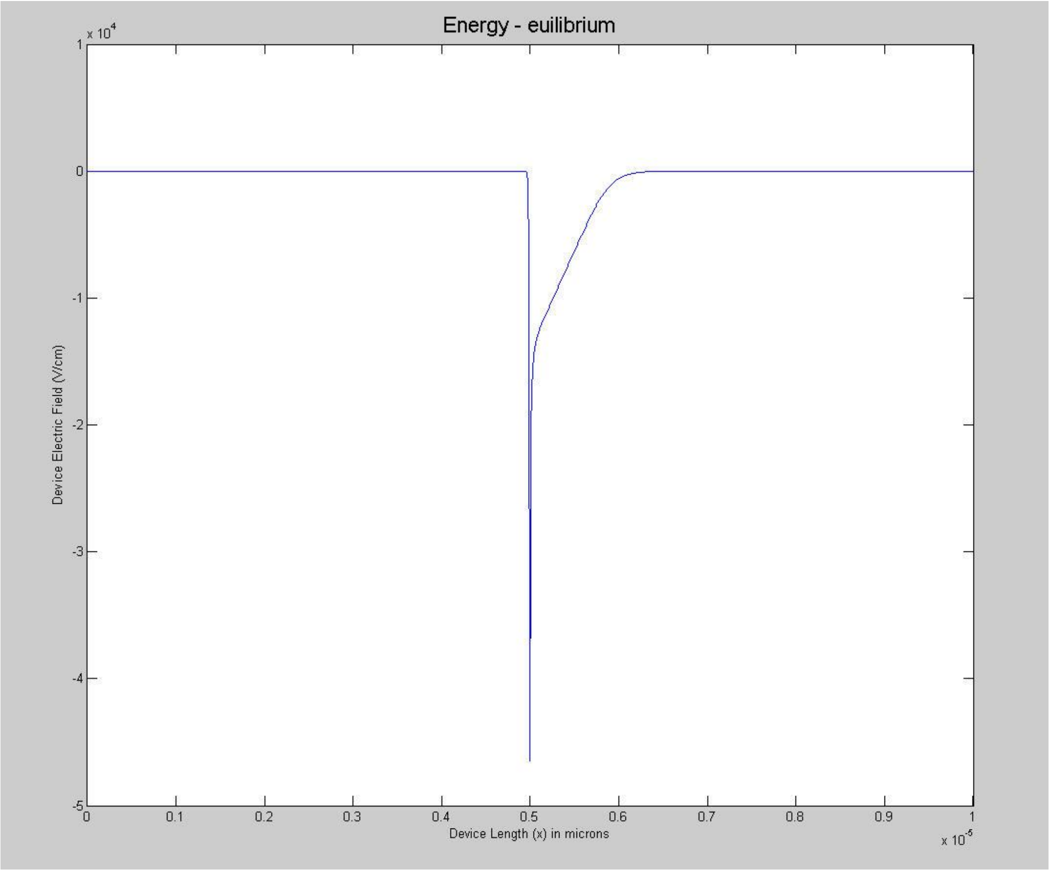

Fig. 9. SDS electric field simulation

5. CONCLUSION

A general purpose semiconductor device simulator (SDS) is developed using MATLAB. The software program developed has provided a tool that can supplement semiconductor device modeling by solving basic semiconductor device equations using MATLAB tools. The use of MALTAB simulation tools made SDS modular in nature and has simplified the numerical analysis and solution algorithms. The program is used to examine device parameters such as carrier statistics, device potential, and internal electric fields. The comparison made with the analytical approximations supports SDS and further strengthen the understanding between theory and numerical solutions and how those solutions were obtained and analyzed.

ACKNOWLEDGEMENTS

Some part of this manuscript was previously presented and published in University of Hawaii International Conferences Science, Technology, Engineering, Math & Education, June 16-18 2014, Honolulu HI: www. Huichawaii .org/ assets/fardi_hamid_-_et_al_stem_2014.pdf

COMPETING INTERESTS

Author has declared that no competing interests exist.

REFERENCES

1. Pinto M, et al. PISCES-II Stanford electronics lab., Dept. of elec. Engr. Stanford Univ., California; 1984.
2. Kurata M. Numerical analysis for semiconductor devices, Lexington, D.C. Heath and Company. 1982;1-4.
3. Atlas user manual. Silvaco International Inc. 2000;1.
4. Mathworks Inc., MATLAB, Sim Windows. 2014;1(1):58.
5. Fardi H, Pace S, Alaghband G. A semiconductor device simulator utilizing MATLAB. University of Hawaii International

Conferences Science, Technology, Engineering, Math & Education, Honolulu HI. 2014;16-18.

6. Winston D. SimWindows-1D semiconductor device simulator. 1999;1:42, Available:www-ocs.colorado.edu/Sim Windows /simwin.html

7. Ivakhno V, Zamaruiev V, Ilina O. Estimation of semiconductor switching losses under hard switching using MATLAB/SIMULINK subsystem. The Scientific Journal of Riga Technical University - Electrical, Control and Communication Engineering. 2013;2.

8. Garg A, Singh RP. Dynamic performance analysis of ig based wind farm with statcom and SVC in MATLAB / SIMULINK. International Journal of Computer Applications, IJCA Journal. 2013;71:23.

9. Wongputorn P, Hullender D, Woods R, King J. Application of MATLAB functions for time domain simulation of systems with lines with fluid transients. J. Fluids Eng. 2005;127(1):177-182. DOI:10.1115/1.185 2488.

10. Ivakhno V, Zamaruiev VV, Ilina O. Stimation of semiconductor switching losses under hard switching using MATLAB/SIMULINK subsystem. Electrical, Control and Communication Engineering. 2013;2(1):20-26. ISSN (Online) 2255-9159, ISSN (Print) 2255-9140. DOI: 10.2478/ecce-2013-0003.

11. Haur T, Kakran S. MATLAB computation for studying effect of location of shunt facts devices in long transmission line system. IJERT. 2013;28-02.

12. Fouda ME, Salama KN, Radwan AG. Effect of boundary on controlled memristor- based oscillator. IEEE International Conference on Engineering and Technology ICET; 2012.

13. Zidan MA, Fahmy H., Hossein MH, Salama KN. Memristor based memory: The sneak paths problem and solutions. Microelectronics Journal. 2013;44(2):176-183.

14. Kumari JS, Babu Ch-Sai. Mathematical modeling and simulation of photovoltaic cell using MATLAB-simulink environment. International Journal of Electrical and Computer Engineering. 2012;2(1):26-34.

15. Du Bin, Hudgins JL, Santi EB, Angus T, Palmer PR, Mantooth HA. Transient electrothermal simulation of power semiconductor devices. IEEE Transactions on Power Electronics. 2010;25(1):237-248. ISSN 0885-8993.

16. Slotboom JW. The pn product in silicon. Solid State Electronics. 1997;20:279-283.

17. Winston D, Hayes RE. SimWindows: A new simulator for studying quantum well optoelectronic devices. Proc. of 21st Annual International Symposium on Compound Semiconductors, San Diego, CA; 1994.

18. Fardi H, Winston D, Hayes RE, Hanna M. Numerical modeling of energy balance equations in AlGaAs/gaAs Qunatum well pin photodiodes. IEEE Transactions on Electron Devices. 2000;ED-47(5):915-921.

19. Horio K, Yanai H. Numerical modelling of heterojunctions including the thermionic emission mechanism at the heterojunction interface. IEEE. 1990;ED-37:1093-1097.

20. Forghieri A, et al. A new discretization strategy of the semiconductor equations comprising momentum and energy balance. IEEE Trans. Computer-Aided Design. 1988;7:231-242.

21. Chen D, Kan EC, Ravaioli U, Yu Z, Dutton RW. A self-consistent discretization scheme for current and energy transport equations proc. IV Int. Conf. Simulation of Semiconductor Devices and Processes (SISPAD) (Zurich). 1991;235-239.

22. Stratton R. Semiconductor current-flow equations (Diffusion and Degeneracy). IEEE Trans. on Electron Devices. 1972;ED-19:1288-1292.

23. Chen D, Yu Z, Wu KC, Goosens R, Dutton RW. Dual energy transport model with coupled lattice and carrier temperatures. Proc. SISDEP V. 1993;125-128.

24. Chen D, Sangiorgi E, Pinto MR, Kan EC, Ravioli U, Dutton RW. Analysis of spurious velocity overshoot in hydrodynamic simulations of ballistic diodes. Proceedings of NUPAD V, Seattle; 1992.

25. Apanovich Y, et al. The influence of lattice heating on semiconductor device characteristics. COMPEL.1993;12:531-539.

26. Apanovich Y, et al. Numerical simulation of submicrometer devices including coupled nonlocal transport and nonisothermal effects. IEEE Trans. on Electron Devices. 1995;42:890-896.

27. Corkish R, Honsberg CB. Numerical modelling of quantum well solar cells. 2nd World Solar Conf. 1997;1-4.

28. Mnatsakanov TT, et al. Carrier mobility model for simulation od SiC-based

electronic devices. Electronic Journal: Semiconductor Science and Technology. 2002;17(9):974-977.

29. Joshi RP. Monte Carlo calculation of the temperature- and field-dependent electron transport parameters for 4H-SiC. J. Appl. Phys. 1995;78(9):5518-5521.
30. Wachutka GK. Rigorous thermodynamic treatment of heat generation and conduction in semiconductor modeling. IEEE Trans. 1990;CAD-9:1141-1149.
31. Apanovich Y, Lyumkis E, Polsky B, Blakey P. An investigation of coupled and decoupled iterative algorithms for energy balance calculations. Proc. SISPAD V. 1993;233-236.
32. Forghieri A, et al. A new discretization strategy of the semiconductor equations comprising momentum and energy balance. IEEE Trans Computer-Aided Design. 1988;7:231-242.

APPENDIX

Semiconductor Device Simulator (SDS)

In this Section, a brief overview of the SDS program is given with explanations for key aspects of the program that are not explicitly covered in any other section. We will begin by looking at the "main" program and then investigate the functions that are implemented in support of the main program.

As we have seen throughout the project, the main purpose is to write a program that solves the matrix-vector equation which was established from the classic differential equations in Section 2. In most aspects the program can be developed however the developer likes, but in certain instances poor coding techniques will lead to longer computation times and ultimately slower convergence speeds for a given device setup. The main important goal is to manipulate the matrix coefficients efficiently and to solve the matrix-vector equation with as little iteration as possible. On key element to this is establishing the proper boundary conditions and trial values.

A basic flow diagram of the main program is given below. The first few blocks simply establish any constants, or numerical parameters required to solve the device. The second block establishes any user defined inputs which also include device information for the device to be simulated. A note should be made that the code provided in Appendix III, and referenced in sections here, is heavily commented and the reader should reference the comments for any confusion that may arise.

```
clear all;  %Clears all previously stored variable information
close all; %Closes all previously open plots
clc;  %Clears the command window to blank
TSTART = tic; %Starts a timer to record solution time
format long eng; %Formats the data to engineering mode
```

This block is a simple setup that is used before any new simulation is run. All stored variable information in the MATLAB workspace is cleared, all open plots are closed, and the command window is cleared. This section also starts a timer, which is used to investigate the speed of the computation algorithm for various device setups.

Every calculated value that is stored in a variable is accessible after the program is run in the main MATLAB workspace. For example, the last iterated value for the error values is stored in an error vector. The program can be easily modified to run through one iteration at a time allowing the user to investigate the change in error over each iteration. Every opportunity for the user to access the calculated data has been provided so that any insight into those variables can be gained if necessary.

Peer-review history:
The peer review history for this paper can be accessed here:
http://www.sciencedomain.org/review-history.php?iid=963&id=22&aid=8080